Cardiac Imaging

Increased ^{99m}Tc-Sestamibi Washout Reflects Impaired Myocardial Contractile and Relaxation Reserve During Dobutamine Stress Due to Mitochondrial Dysfunction in Dilated Cardiomyopathy Patients

Daisuke Hayashi, MD,*† Satoru Ohshima, MD, PhD,*‡ Satoshi Isobe, MD, PhD,*
Xian Wu Cheng, MD, PhD,* Kazumasa Unno, MD, PhD,* Hidehito Funahashi, MD, PhD,*‡
Norihiro Shinoda, MD,* Takahiro Okumura, MD, PhD,* Akihiro Hirashiki, MD, PhD,*
Katsuhiko Kato, MD, PhD,§ Toyoaki Murohara, MD, PhD*

Nagoya, Kagamigahara, and Tsushima, Japan

Objectives   This study investigated whether the technitium-99m sestamibi (MIBI) washout rate (WR) would predict mitochondrial damage and myocardial dysfunction in patients with dilated cardiomyopathy (DCM).

Background   Myocardial mitochondrial damage reduces adenosine triphosphate production, resulting in myocardial dysfunction. Increased myocardial ^{99m}Tc-MIBI washout is reportedly caused by mitochondrial dysfunction.

Methods   Twenty DCM patients (New York Heart Association functional class I–III) underwent myocardial ^{99m}Tc-MIBI scintigraphy and cardiac catheterization. Myocardial MIBI uptake was quantified as an early and delayed heart-to-mediastinum ratio, and WR was calculated. Maximum first derivative of left ventricular (LV) pressure (LV dP/dt$_{max}$) (an index of myocardial contractility) and LV pressure half-time (T$_{1/2}$) (an index of myocardial relaxation) were calculated by the left ventricular pressure curve at baseline and during dobutamine infusion (15 μg/kg/min at maximum). Endomyocardial biopsy specimens were obtained for quantitative mRNA analysis and electron microscopy. The patients were divided into two groups as follows: 1) group A of 10 patients showing a WR ≤24.3% (median value) and 2) group B of 10 patients showing a WR >24.3%.

Results   WR was significantly correlated with the percentage changes in LV dP/dt$_{max}$ (%LV dP/dt$_{max}$) (r: −0.59; p = 0.01) and T$_{1/2}$ (r: −0.57; p = 0.03) from baseline to peak dobutamine stress. The %LV dP/dt$_{max}$ was significantly greater in group B than in group A. The abundance of mRNAs for mitochondrial electron transport–related enzymes was more significantly reduced in group B than in group A. Electron microscopy revealed significant correlations between WR and the severity of mitochondrial damage (r: 0.88; p = 0.048) and glycogen accumulation (r: 0.90; p = 0.044).

Conclusions   Increased ^{99m}Tc-MIBI washout may predict mitochondrial dysfunction and the impairment of myocardial contractile and relaxation reserves during dobutamine stress in DCM patients.   (J Am Coll Cardiol 2013;61:2007–17) © 2013 by the American College of Cardiology Foundation

Dilated cardiomyopathy (DCM) is characterized by left ventricular (LV) dilatation and myocardial systolic dysfunction (1,2). The recent advancement in pharmacological treatments, such as treatments with renin-angiotensin-aldosterone system inhibitors or beta-blockades, provides

significant beneficial effects for patients with DCM. However, some DCM patients fail to show significant responses to these treatments, resulting in a poor prognosis. The prevalence of severe myocardial damage, including mito-

chondrial functional failure, is thought to be associated with a poor prognosis. Accordingly, it is important to clarify the underlying pathophysiological mechanisms involved in refractoriness to any treatments.

Myocardial technitium-99m–labeled sestamibi (MIBI) is commonly used as a myocardial perfusion imaging tracer for

detecting significant coronary artery disease. Approximately 90% of myocardial MIBI is localized within a mitochondrial fraction. Myocardial MIBI uptake, which is positively charged electrically, depends on a strong negative charge in mitochondrial membranes (3,4). A lack of MIBI uptake has been reported in some experimental studies (5,6). In addition, an increased MIBI washout is thought to be related to impaired mitochondrial function coexisting with myocardial damage (7,8). An increased myocardial MIBI washout was often reported in patients with myocardial infarction (9,10) or cardiomyopathy (11–14). We previously reported that increased MIBI washout was associated with abnormal myocardial properties linked to myocardial mitochondrial damage in patients with nonobstructive hypertrophic cardiomyopathy (15,16).

In the present study, we investigated the relationship between myocardial MIBI washout, myocardial functional properties, mitochondrial messenger ribonucleic acid (mRNA) expression, and mitochondrial structural configuration in DCM patients.

Methods

Study population. A total of 20 DCM patients (11 men and 9 women; mean age: 50 ± 13 years; and mean LV ejection fraction [LVEF]: $34 \pm 9\%$) were studied. DCM was diagnosed on the basis of clinical, electrocardiographic and echocardiographic findings according to previously proposed diagnostic criteria (17). Patients were excluded if they showed prior evidence of coronary artery disease, primary valvular disease, essential or secondary hypertension, chronic atrial fibrillation, or diabetes mellitus. All patients underwent coronary angiography to exclude those with significant coronary artery disease. An endomyocardial biopsy was also performed to assess the reverse transcriptase–polymerase chain reaction (RT-PCR) analysis, and electron microscopy was subsequently conducted. All patients underwent cardiac catheterization analysis at rest and under dobutamine stress, as well as myocardial MIBI scintigraphy at rest. The study protocol was approved by the ethics review board at the Nagoya University School of Medicine, and written informed consent was obtained from all patients.

Myocardial MIBI scintigraphy. Myocardial MIBI scintigraphy was conducted at rest. Six hundred megabecquerels of MIBI tracer was injected in each patient intravenously. The initial images were acquired 60 min after tracer injection, and the delayed images were initiated 4 h later. A Toshiba gamma triple-head rotation camera (GCA9300, Toshiba Inc., Tokyo, Japan) equipped with a low-energy, high-resolution collimator was used for single-photon emission computed tomography (SPECT) imaging. Projection images were obtained over a 360° arc at an acquisition time of 20 s per image. A 20% symmetric window centered at 140 KeV was applied. Projected image data were transferred to a dedicated computer using a 64×64 matrix size. For SPECT reconstruction, Butterworth filter served as prefilter and Ramp filter as back-projection filter, with a cutoff frequency of 0.32 cycles/pixel and an order of 8, were used without correction for attenuation or scatter. Tomographic slices were reconstructed relative to the anatomic axis of the left ventricle. The vertical and horizontal long-axis and short-axis slices were then generated.

For quantitative analysis, the early and delayed heart-to-mediastinal ratio (H/M) and global WR were calculated. The region of interest (ROI) on the planar imaging was manually set over the whole heart and a rectangular ROI on the upper mediastinum. The H/M was calculated as (Count density of the whole LV)/(Count density of the mediastinum). The global WR was also calculated on the planar image as [(Initial H−Initial M)−(Delayed H−Delayed M) × DC]/(Initial H−Initial M) × 100, where H indicates mean heart counts, M indicates mean mediastinal counts, and DC indicates decay coefficiency. The normal values of MIBI WR, early H/M, and delayed H/M of the age-matched control group (10 subjects; 9 men; age: 56 ± 9 years; LVEF: $70 \pm 7\%$) were $11 \pm 5\%$, 3.5 ± 0.3, and 3.1 ± 0.3, respectively.

Echocardiography. Echocardiography was performed using a Sonos 2500 ultrasound system (Hewlett-Packard, Andover, Massachusetts) equipped with a 2.5- to 3.5-MHz transducer. The LV end-diastolic dimension, LV end-systolic dimension, interventricular septal thickness, posterior wall thickness, and LVEF were measured on the M-mode of the long-axis image according to standard criteria recommended by the American Society of Echocardiography (18).

Cardiac catheterization and endomyocardial biopsy. Biventricular catheterization was performed using the standard techniques. In the left heart catheter, a 6-F fluid-filled pigtail catheter with a high-fidelity micromanometer (CA-61000-PLB Pressure-tip Catheter; CD Leycom, Zoetermeer, the Netherlands) was positioned in the left ventricle for the measurement of LV pressure. Micromanometer pressure signals and standard electrocardiograms were continuously recorded with a multichannel recorder online. The LV pressure signals were digitized at 3-ms intervals and

were analyzed throughout the procedure with software developed in-house and a 32-bit microcomputer system. The LV pressure and heart rate (HR) were determined as averages of at least 15 consecutive beats. The LV end-diastolic pressure, the maximum first derivative of LV pressure (LV dP/dt$_{max}$) as an index of contractility, and the LV pressure half-time (T$_{1/2}$) as an index of LV isovolumic relaxation were measured both at baseline and under dobutamine stress as previously described (19,20). In the right heart catheter, a 7-F triple-lumen Swan-Ganz thermodilution catheter was positioned in the right pulmonary artery to measure the pulmonary arterial wedge pressure and cardiac index. For a pharmacological stress test, dobutamine was intravenously injected with an infusion pump at a starting dose of 5 μg/kg/min, followed by incremental doses of 10 μg/kg/min and 15 μg/kg/min as previously described (19,20). The percentage changes in the LV dP/dt$_{max}$ (%LV dP/dt$_{max}$) and T$_{1/2}$ (%T$_{1/2}$) from the baseline to peak values under dobutamine stress were also calculated.

An endomyocardial biopsy was performed on all patients to exclude myocarditis (according to the Dallas criteria) as well as specific heart muscle diseases detected by an electron microscopic analysis. Biopsy specimens were obtained from the septum of the right ventricle with a 6-F bioptome. The tissue was fixed immediately in 10% buffered formalin and embedded in paraffin. Three or four specimens were analyzed for each patient.

RT-PCR. Total mRNA was isolated from 1 to 2.5 mg of frozen biopsy specimens of all patients with the use of an RNeasy Fibrous Tissue Mini-Kit (Qiagen, Valencia, California). The RNA was subjected to reverse transcription with an RNA PCR Core Kit (Applied Biosystems, Foster City, California), and the resulting cDNA was subjected to quantitative PCR analysis with an ABI 7300 Real-Time PCR System (Applied Biosystems) as previously described (21). The sequences of primers and TaqMan probes specific to the human alpha-ketoglutarate dehydrogenase (α-KGDH), nicotinamide adenine dinucleotide (NADH) dehydrogenase (ubiquinone) flavoprotein 3 (NDUFV3) (complex I), cytochrome c oxidase subunit 5B (COX5B) (respiratory complex IV), P-glycoprotein, and glyceraldehydes-3-phosphate dehydrogenase (GAPDH) were described previously (15). The amount of mitochondrial protein mRNAs in endomyocardial biopsy specimens was determined by RT-PCR analysis and was normalized relative to that of GAPDH mRNA.

Electron microscopic analysis of myocardial mitochondria. Electron microscopy was performed on six patients (four patients of group A and two patients of group B). Biopsy samples were cut into ~1-mm^3 slices, and were fixed first for 24 h with 2% glutaraldehyde in 0.16 M sodium phosphate (pH 7.2) and then for 1 h with 1% osmium tetroxide. The fixed tissues were dehydrated in a graded series of ethanol solutions before exposure to propylene oxide and embedding in Epon. Sections were cut at a thickness of 60 to 70 nm, stained with uranyl acetate and lead citrate, and observed with a JEM-1400 transmission electron microscope (JEOL, Tokyo, Japan) operating at 100 kV. The quantitation of mitochondrial numbers and sizes was performed at a magnification of 8,000$\times$ by counting the corresponding number of pixels using Adobe Photoshop version 7.0.1. A total of 120 mitochondrial cross-sectional areas from six sections were measured for each patient, and histograms were generated separately for each group of patients.

The severity of the mitochondria degeneration was analyzed, and the mitochondria were examined in accordance with the severity of the degeneration of cristae, as follows: the mitochondria with a normal form were denoted as *A*; those with 1% to 25% of degenerated cristae, *B*; those with 26% to 50%, *C*; those with 51% to 75%, *D*; and those with 76% to 100%, *E*. Each fraction of mitochondria was counted in one field of view six times and averaged for each patient. Finally, a mitochondria damage index (MDI) was calculated as follows:

$$\text{MDI} = 1 \times a/100 + 2 \times b/100 + 3 \times c/100 + 4 \times d/100 + 5 \times e/100$$
$$(\text{A}:1 \text{ point}; \text{a } \%, \text{B}:2 \text{ points}; \text{b } \%,$$
$$\text{C}: 3 \text{ points}; \text{c } \%, \text{D}:4 \text{ points}; \text{d } \%, \text{E}:5 \text{ points}; \text{e } \%)$$

The glycogen accumulation and lipid droplets were also counted and averaged in the same way.

Blood sampling. Each blood sample was immediately placed on ice and centrifuged at 4°C. The plasma levels of neurohumoral factors, such as norepinephrine, epinephrine, brain natriuretic peptide (BNP), renin, and aldosterone, were also measured. Plasma norepinephrine levels were measured using high-performance liquid chromatography. Plasma BNP levels were measured with a specific radioimmunoassay for human BNP.

Patient classification. Patients were classified into two groups according to the median value of WR, as follows: group A consisted of 10 patients showing a WR of ≤24.3% (a median value of WR); group B consisted of 10 patients showing a WR of >24.3%.

Statistical analysis. Data were presented as the mean ± SD or the median value (quartiles 1–3). Comparisons of data between the two groups were analyzed using the Student *t* test, whereas BNP, epinephrine, renin, and aldosterone, which were not normally distributed, were compared with a nonparametric Mann-Whitney *U* test. The fractions of sex, New York Heart Association (NYHA), and medications between the 2 groups were compared with a chi-square test or a Fisher exact test as appropriate. The relationship of each parameter was determined using Spearmen's rank correlation coefficients. A p of <0.05 was considered statistically significant.

Results

Patient characteristics. The patient characteristics are presented in Table 1. Their mean age was 50 ± 13 years. Eight

Table 1	Patient Characteristics
Age, yrs	50 ± 13
Sex	
Male	11
Female	9
NYHA functional class	
I	8
II	10
III	2
Echocardiography	
LVEF (%)	33 ± 11
LVDd (mm)	64 ± 7
LVDs (mm)	52 ± 9
IVST (mm)	9 ± 2
LVPWT (mm)	10 ± 3
E/A	1.1 ± 0.4
DcT (ms)	281 ± 28
Cardiac catheterization	
LVEDP (mm Hg)	16.5 ± 9.6
PAWP (mm Hg)	12.2 ± 6.9
CO (l/min)	5.1 ± 0.9
CI (l/min/m²)	2.8 ± 0.6
Neurohumoral factors (pg/ml)	
BNP	74 (51–306)
Epinephrine	34 (2–43)
Norepinephrine	671 ± 41
Renin	14 (8–19)
Aldosterone	192 (12–228)
Myocardial scintigraphy	
Early H/M	2.8 ± 0.5
Delayed H/M	2.9 ± 0.6
WR (%)	24.4 ± 8.4

Values are mean ± SD, n, or median (quartiles 1−3).

BNP = brain natriuretic peptide; CI = cardiac index; CO = cardiac output; DcT = deceleration time; E/A = E to A wave ratio; H/M = heart-to-mediastinal ratio; IVST = interventricular septal thickness; LVDd = left ventricular end-diastolic dimension; LVDs = left ventricular end-systolic dimension; LVEDP = LV end-diastolic pressure; LVEF = left ventricular ejection fraction; LVPWT = LV posterior wall thickness; NE = norepinephrine; NYHA = New York Heart Association; PAWP = pulmonary arterial wedge pressure; WR = washout rate.

patients were classified as NYHA functional class I, 10 patients as NYHA class II, and 2 patients as NYHA class III. The mean early and delayed H/Ms were 2.8 ± 0.5 and 2.9 ± 0.5, respectively. The mean and median values of WR were 24.4 ± 8.4% and 24.3%, respectively. The LV end-diastolic diameter and LV end-systolic diameter derived from echocardiography were 64 ± 7 mm and 52 ± 9 mm, respectively, suggesting LV dilation. The interventricular septal thickness and posterior wall thickness were 9 ± 2 mm and 10 ± 3 mm, respectively. The LVEF was reduced to a mean value of 33 ± 11%. The plasma BNP and norepinephrine levels were 74 (51 to 306) pg/ml and 671 ± 41 pg/ml, respectively, suggesting elevated neurohumoral factors.

Comparison of parameters between 2 groups. Comparisons of parameters are presented in Table 2. The LV end-diastolic diameter (67 ± 8 mm vs. 60 ± 4 mm; p = 0.04) and end-systolic diameter (57 ± 10 mm vs. 47 ± 5 mm; p = 0.002) were significantly greater in group B than in group A. The plasma levels of noradrenaline were more

significantly elevated in group B than in group A (862 ± 420 pg/ml vs. 457 ± 286 pg/ml; p = 0.03).

Relationship between MIBI WR and hemodynamic changes. The baseline values of LV dP/dt_{max} and $T_{1/2}$ were similar in the two groups. The peak values of LV dP/dt_{max} at 15 μg/kg/min of dobutamine stress, and %LV dP/dt_{max} were significantly lower in group B than in group A (1,757 ± 703 mm Hg/s vs. 3,160 ± 1,238 mm Hg/s [p = 0.02] and 87 ± 42% vs. 148 ± 56% [p = 0.004], respectively). The %$T_{1/2}$ tended to be lower in group B than in group A (37 ± 15% vs. 48 ± 9%; p = 0.08) (Table 2).

Although the MIBI WR did not significantly correlate with the baseline LV dP/dt_{max} and $T_{1/2}$, it did significantly correlate with the %LV dP/dt_{max} and %$T_{1/2}$ (r: −0.59 [p = 0.01] and r: −0.57 [p = 0.03], respectively) (Fig. 1). No significant correlations were observed between early or delayed H/M and %LV dP/dt_{max} or %$T_{1/2}$.

Expression of mitochondria mRNA. The abundance of mRNAs for mitochondrial electron transport−related enzymes, such as α-KGDH, NDUFV3, and COX5B, was significantly lower in group B than in group A (0.43 ± 0.21 vs. 0.95 ± 0.40 [p < 0.0001]; 0.52 ± 0.21 vs. 1.24 ± 0.47 [p < 0.0001]; and 0.45 ± 0.14 vs. 0.95 ± 0.37 [p = 0.0003], respectively) (Fig. 2). Significant inverse correlations were noted between MIBI WR and α-KGDH/GAPDH, NDUFV3/GAPDH, and COX5B/GAPDH (r: −0.78 [p = 0.0006]; r: −0.76 [p = 0.001]; and r: −0.62 [p = 0.007], respectively), whereas no significant correlation was seen between MIBI WR and P-glycoprotein/GAPDH (Fig. 3).

Relationship between MIBI WR and electron microscopic findings. Ventricular biopsy specimens from 6 patients (4 patients of group A and 2 patients of group B) were available for electron microscopic analysis. A significant correlation was observed between MIBI WR and MDI (r: 0.88; p = 0.048), but none was observed between MIBI WR and the total number of mitochondria (Fig. 4A). A significant correlation was found between the MIBI WR and glycogen-positive areas (r: 0.90; p = 0.044), whereas none was observed between MIBI WR and lipid droplets (Fig. 4B).

Case presentation. Two typical cases are shown in Figure 5. Figure 5A shows a 66-year-old man without a globally increased MIBI WR and with a favorably increased %LV dP/dt_{max} and a relatively preserved mitochondrial configuration and small areas of glycogen accumulations in electron microscopy. Figure 5B shows a 45-year-old woman with an increased global MIBI WR, a gentle increase in %LV dP/dt_{max} in response to dobutamine, and numerous damaged mitochondria and glycogen and lipid droplets on electron microscopy.

Discussion

The present study demonstrated that an increased myocardial MIBI washout was correlated with a decrease in myocardial mitochondrial mRNA expression or an abnormal morphology of mitochondria in patients with DCM. In

Table 2	Comparison of Each Parameter Between Groups A and B		
Parameter	**Group A (n = 10)**	**Group B (n = 10)**	**p Value**
Age (yrs)	51 ± 15	48 ± 10	0.61
Sex			0.054
Male	7	4	
Female	3	6	
NYHA functional class			—
I	4	4	
II	6	4	
III	0	2	
BMI (kg/m^2)	25.3 ± 4.3	25.9 ± 5.7	0.80
Echocardiography			
LVEF (%)	37 ± 7	31 ± 10	0.12
LVDd (mm)	60 ± 4	67 ± 8	0.04
LVDs (mm)	47 ± 5	57 ± 10	0.002
IVST (mm)	10 ± 3	8 ± 2	0.14
LVPWT (mm)	11 ± 4	9 ± 2	0.23
E/A	0.9 ± 0.3	1.2 ± 0.4	0.15
DcT (ms)	210 ± 55	208 ± 65	0.96
Myocardial scintigraphy			
Early H/M	3.0 ± 0.5	2.8 ± 0.5	0.40
Delayed H/M	3.2 ± 0.5	2.8 ± 0.6	0.19
Neurohumoral factors (pg/ml)			
BNP	74 (32–125)	160 (53–312)	0.27
Epinephrine	25 (20–37)	37 (29–47)	0.36
Norepinephrine	457 ± 286	862 ± 420	0.03
Renin	14 (7–17)	15 (9–32)	0.49
Aldosterone	146 (122–244)	206 (126–226)	0.95
Medication			
Diuretic	7	5	0.21
Beta-blocker	8	6	0.20
ACE-I or ARB	8	6	0.20
Statin	1	1	1.00
Cardiac catheterization			
LV dP/dt$_{max}$ (mm Hg/s)			
Baseline	1,228 ± 397	961 ± 302	0.11
DOB 5 μg/kg/min	1,723 ± 734	1,199 ± 465	0.08
DOB 10 μg/kg/min	2,364 ± 1,139	1,574 ± 610	0.09
DOB 15 μg/kg/min	3,160 ± 1,238	1,757 ± 703	0.01
%Δ			
DOB 5 μg/kg/min	40 (25–48)	14 (9–27)	0.16
DOB 10 μg/kg/min	84 ± 53	62 ± 31	0.30
DOB 15 μg/kg/min	148 ± 56	87 ± 42	0.02
T$_{1/2}$ (ms)			
Baseline	41.6 ± 5.3	42.9 ± 11.3	0.75
DOB 5 μg/kg/min	36.5 ± 8.7	38.0 ± 11.7	0.75
DOB 10 μg/kg/min	27.8 ± 5.5	31.4 ± 12.6	0.43
DOB 15 μg/kg/min	21.3 ± 3.9	28.9 ± 11.6	0.09
%Δ			
DOB 5 μg/kg/min	13 (4–23)	10 (3–21)	0.93
DOB 10 μg/kg/min	31 ± 15	28 ± 14	0.73
DOB 15 μg/kg/min	48 ± 9	37 ± 15	0.08
LVEDP (mm Hg)	16.8 ± 7.1	16.1 ± 12.1	0.88
PAWP (mm Hg)	11.3 ± 5.5	13.0 ± 8.3	0.60
CO (l/min)	5.1 ± 1.0	5.1 ± 1.0	0.96
CI (l/min/m^2)	2.8 ± 0.5	2.9 ± 0.6	0.64

Values are mean ± SD, n, or Median (quartiles 1−3).

ACE-I = angiotensin-converting enzyme inhibitor; ARB = angiotensin II receptor blocker; BMI = body mass index; DOB = dobutamine; LV dP/dt$_{max}$ = maximum first derivative of LV pressure; T$_{1/2}$ = LV pressure half-time; other abbreviations as in Table I.
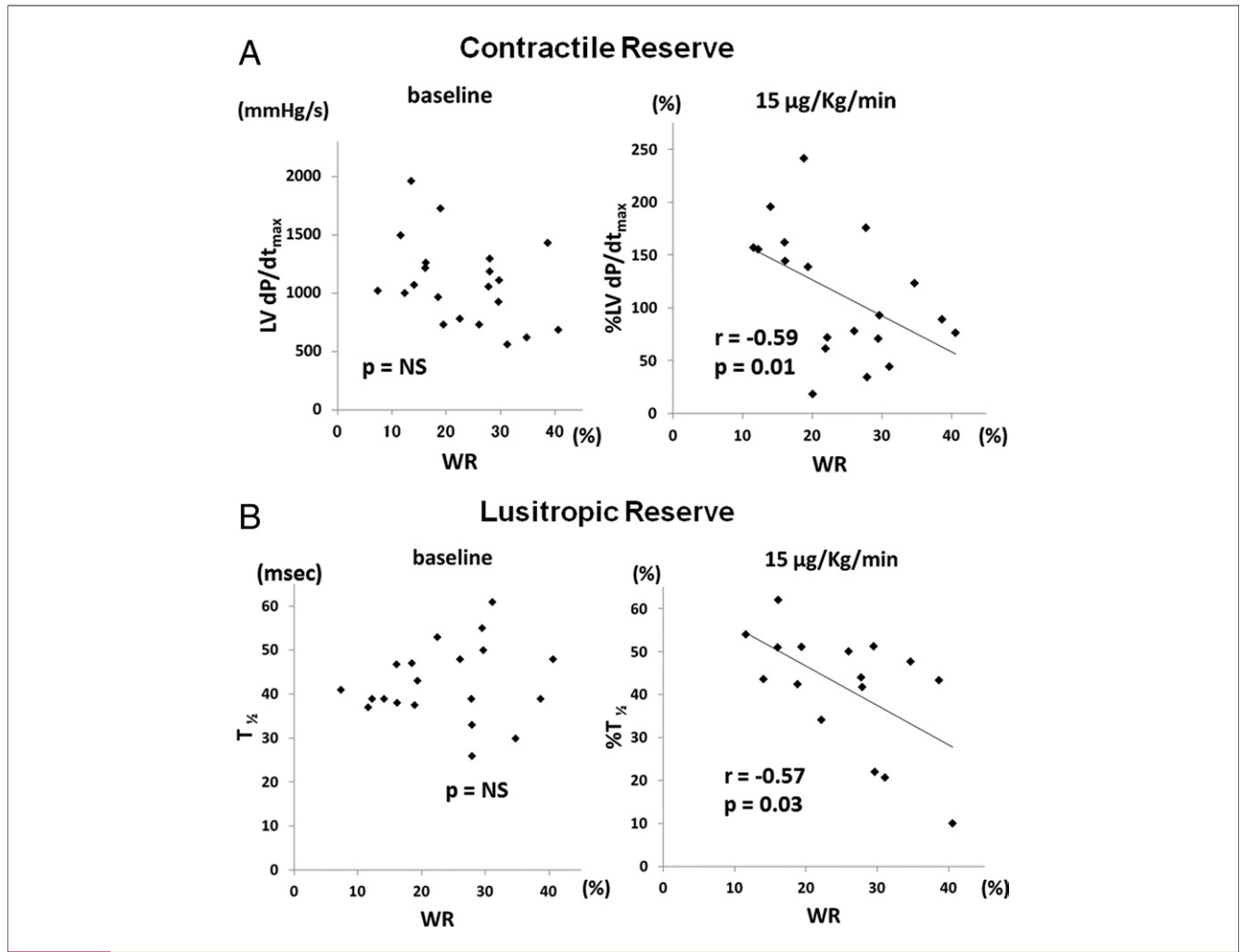
Figure 1   Relationship Between MIBI WR and Hemodynamic Changes From Baseline to Peak Dobutamine Stress

(A) A significant inverse correlation was observed between technitium-99m sestamibi (MIBI) washout rate (WR) and percentage changes (%) in maximum first derivative of LV pressure (LV dP/dt$_{max}$) from baseline to peak (15 μg/kg/min) dobutamine stress. **(B)** A significant inverse correlation was observed between MIBI WR and % changes in LV pressure half-time (T$_{1/2}$) from baseline to peak (15 μg/kg/min) dobutamine stress.

addition, a myocardial MIBI washout was also correlated with an impairment in the myocardial contractile and relaxation reserves.

An increased myocardial MIBI washout is thought to reflect an impairment in mitochondrial function as a result of a decrease in the mitochondrial transmembrane potential (4,7). In the present study, we examined the expression of several mitochondrial protein mRNAs involved in the myocardial ATP production of DCM patients. Mitochondrial ATP production is mainly generated by the tricarboxylic acid cycle (TCA cycle) in the mitochondrial matrix and the electron transport chain in the mitochondrial membrane. α-KGDH is a key enzyme in the production of NADH by the TCA cycle and regulates the mitochondrial electron transport system (22). NADH$-$ubiquinone oxidoreductase (complex I) and cytochrome c oxidase (complex IV) are the main components that remove protons in the mitochondrial respiratory chain. Abnormalities of the mi-

tochondrial respiratory chain were detected in patients with heart failure and were attributed to a reduction in the activity rates of the electron transport chain (23). Electron transportation is accompanied by the phosphorylation of adenosine diphosphate by the movement of protons though the inner mitochondrial membrane from the matrix to the intermembrane space. This process generates an electrical gradient across the inner mitochondrial membrane, which has a more negative potential on the inside than on the outside of the membrane. In the present study, MIBI WR inversely correlated with the abundance of mRNA expression in α-KGDH, NDUFV3, and COX5B. These findings may suggest that the production of NADH by α-KGDH, as well as that of NADH by NDUFV3 or COX5B, plays a very important role in these enzymes on energy metabolism. A decrease in mitochondrial enzyme gene expression was associated with a reduction in the mitochondrial transmembrane potential (24,25), which affects the mitochondrial
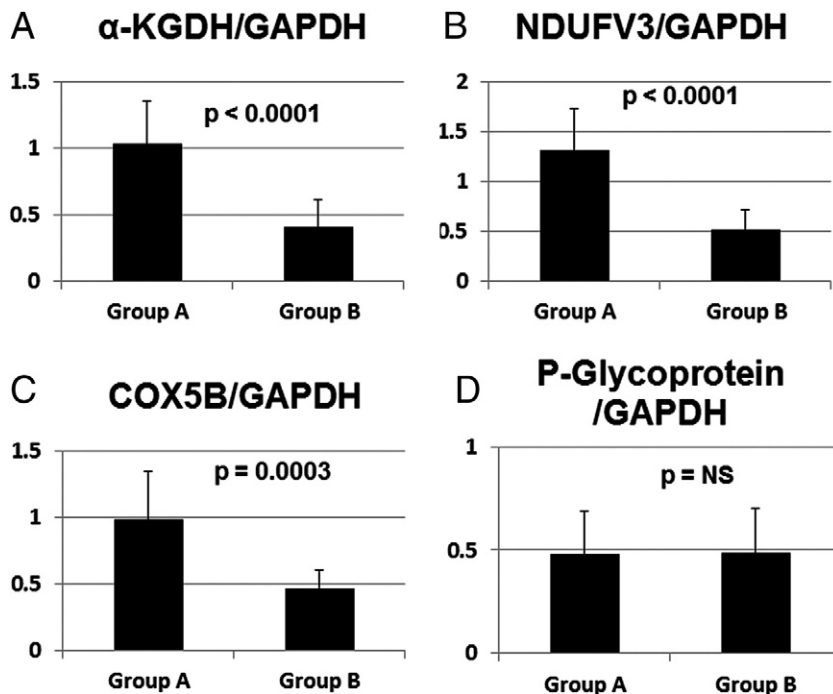
Figure 2   Comparison of Mitochondrial mRNA Expression Between the 2 Groups

(A to D) Alpha-Ketoglutarate dehydrogenase (α-KGDH), nicotinamide adenine dinucleotide dehydrogenase-ubiquinone flavoprotein 3 (NDUFV3), and cytochrome c subunit 5B (COX5B) were significantly lower in group B than in group A.
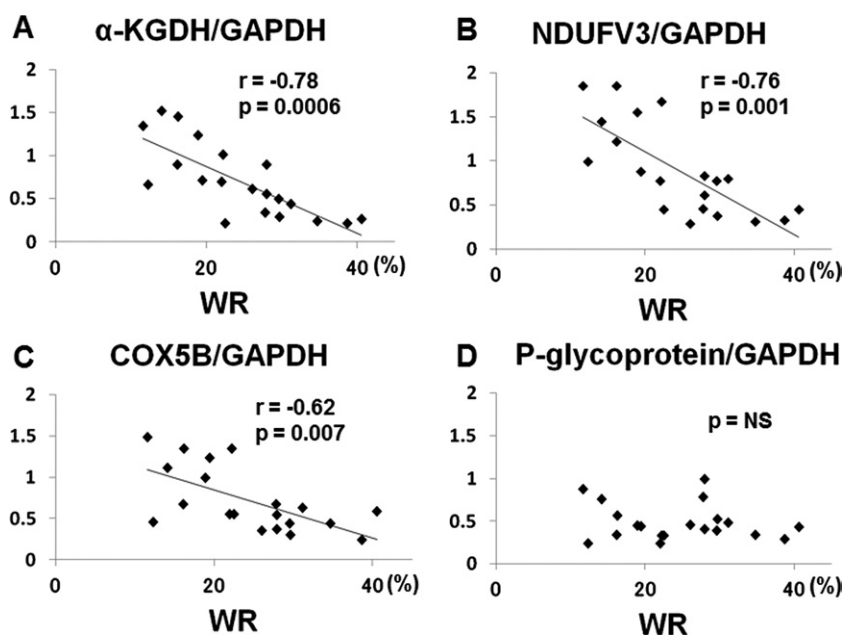
Figure 3   Relationship Between MIBI WR and Expression of Mitochondrial mRNA

(A to D) Significant inverse correlations were observed between MIBI WR and α-KGDH/glyceraldehyde-3-phosphate dehydrogenase (GAPDH), NAUFV3/GAPDH, or COX5B/GAPDH. Abbreviations as in Figures 1 and 2.
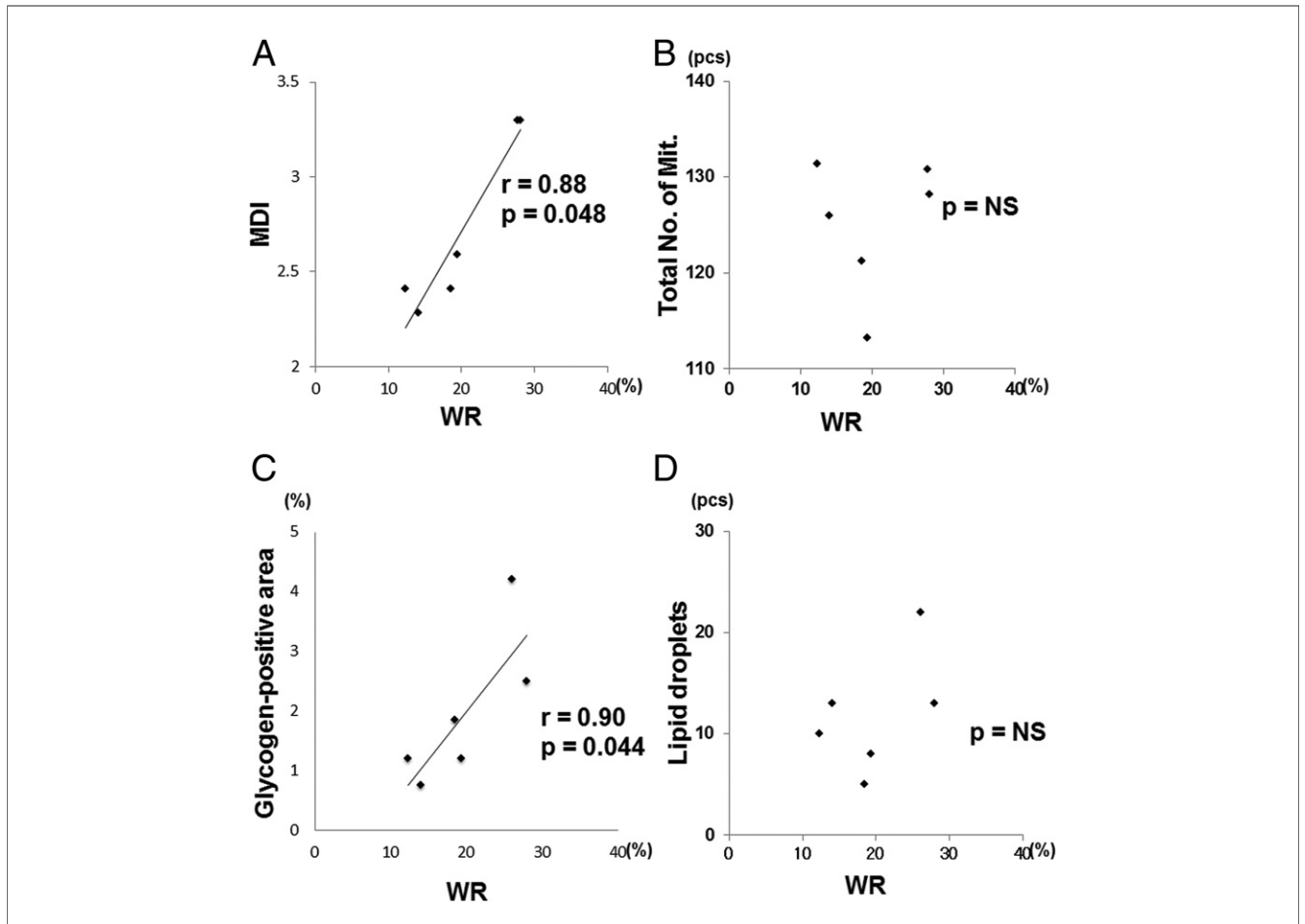
**Figure 4   Relationship Between MIBI WR and Parameters of Electron Microscopic Findings**

Significant correlations were observed between MIBI WR and **(A)** the mitochondria damage index (MDI) and **(C)** glycogen-positive areas,
whereas no significant correlation was seen between MIBI WR and **(B)** total number of mitochondria or **(D)** lipid droplets. Mit. = mitochondria;
other abbreviations as in Figure 1.

function. Those abnormalities may be attributed to an increased MIBI washout observed in our study.

Our electron microscopic findings revealed that the severity of degeneration in the cristae of mitochondria in the myocardium was correlated with myocardial MIBI WR. On the other hand, no significant relationship was seen between the numbers of mitochondria and MIBI WR. Our previous electron microscopic study in patients with hypertrophic cardiomyopathy demonstrated that the number of mitochondria and the variance in mitochondrial size were increased in patients with an impaired myocardial contractile or relaxation reserve (15). Overproliferated and premature mitochondria exhibit an inappropriate ATP production, which would result in the impairment of myocardial contractile or relaxation reserves in patients with hypertrophic cardiomyopathy. The present study did not show the number of changes in mitochondria, but showed instead the ultrastructural abnormalities of mitochondria, which may lead to myocardial dysfunction in DCM patients. Moreover, we observed an increased accumulation of glycogen in

some DCM patients, and the glycogen accumulations were correlated with myocardial MIBI WR. Furthermore, an increased glycogen accumulation was more frequently observed in the areas around severely degenerated and disorganized mitochondria. These findings were in accordance with the results previously demonstrated—that an increased glycogen accumulation was induced by an impaired ATP utilization in patients with more advanced cardiomyopathy (15,21,26). In addition, though lipid accumulation was frequently observed in all patients, it did not correlate with myocardial MIBI WR. Lipid accumulation in the myocardium would reflect the abnormality of lipid metabolism. An increased lipid accumulation in the myocardium results in lipotoxicity, leading consequently to cardiomyocyte apoptosis (27).

In the present study, the baseline parameters of echocardiography or cardiac catheterization did not correlate with myocardial MIBI WR, but rather with the percentage changes in an index of myocardial contractility or relaxation. Moreover, myocardial MIBI WR was inversely correlated
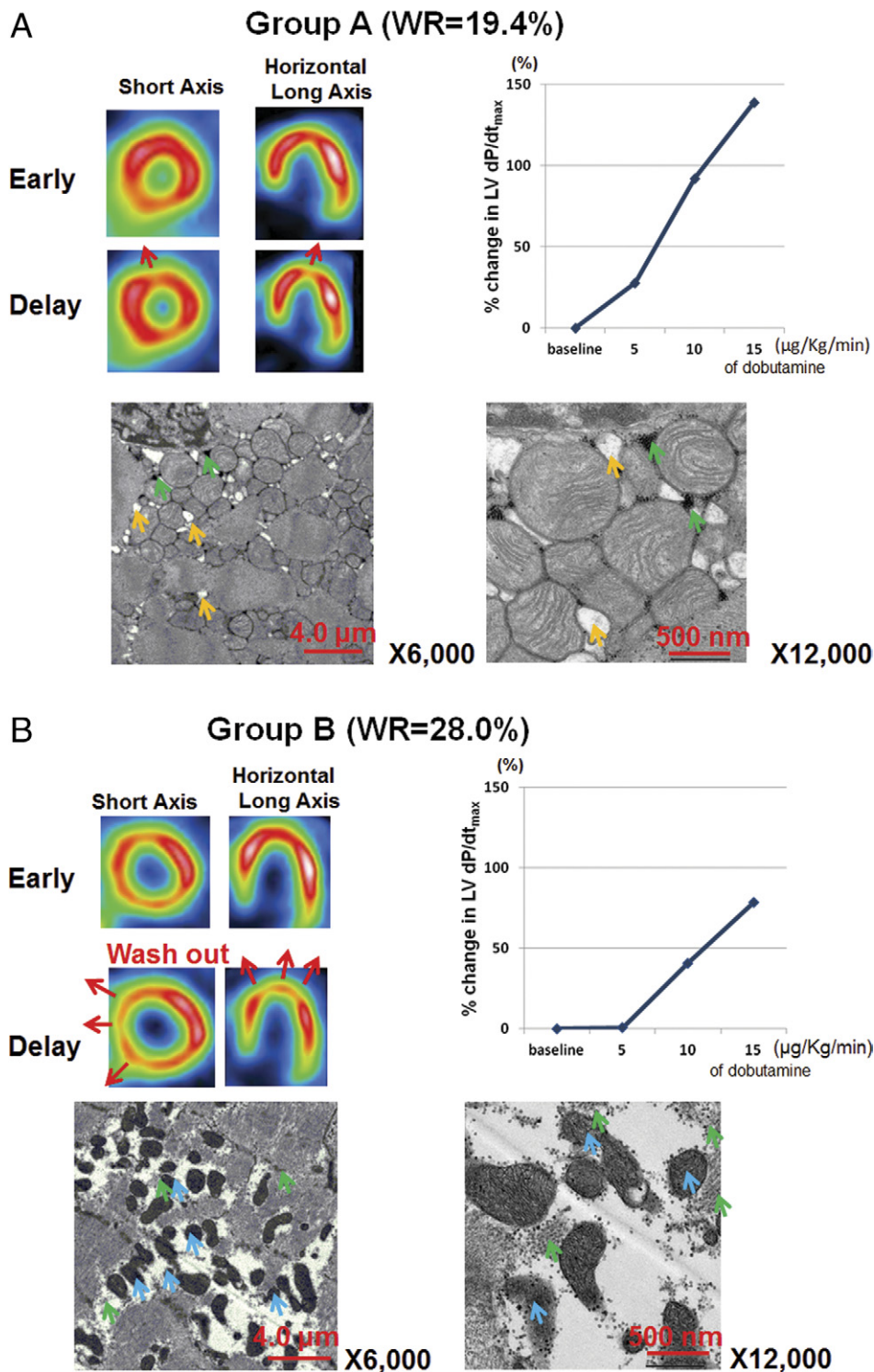
Figure 5   Representative Case of Each Study Group

Two typical cases are presented. **(A)** A 66-year-old man shows no global increased MIBI WR (19.4%). An increased washout was observed in the small anteroapical area **(red arrows)** on MIBI single-photon emission tomography (SPECT). The %LV dP/dt$_{max}$ was favorably increased (5 μg/kg/min: 28%; 10 μg/kg/min: 92%; 15 μg/kg/min: 139%). Electron microscopy revealed a relatively preserved mitochondrial configuration as well as a small amount of glycogen accumulations **(green arrows)** and lipid droplets **(yellow arrows)**. **(B)** A 45-year-old woman exhibited an increased MIBI WR (28.3%). An increased washout was particularly observed in the anteroseptal to the inferoseptal wall on MIBI SPECT. The %LV dP/dt$_{max}$ showed a subtle increase in response to dobutamine (5 μg/kg/min: 0.5%; 10 μg/kg/min: 41%; 15 μg/kg/min: 78%). Electron microscopy revealed many damaged mitochondria **(blue arrows)** and glycogen accumulations **(green arrows)**. Abbreviations as in Figure 1.

with myocardial contractile reserves during dobutamine stress. An impairment in myocardial contractile reserves has been frequently reported to be an important predictor for prognosis or detecting responder to medical therapy in DCM patients (28,29). It is reported that an impairment of the myocardial reserve is related to the abnormalities of Ca^{2+}-handling or to an impairment of the mitochondrial respiratory process in cardiomyopathy patients (15,19,30). Our results demonstrating that myocardial MIBI WR reflects an impairment in myocardial functional reserves and mitochondrial dysfunction or structural abnormalities may provide a clue to better understanding the pathophysiological mechanisms underlying the refractoriness to medical treatments or poor prognoses in DCM patients. Myocardial MIBI scintigraphy may prove to be a useful tool for a noninvasive assessment of the prognosis in DCM patients.
Study limitations. The patient population was very small, resulting in the absence of a significant correlation between MIBI WR and the baseline LV dP/dt_{max} or $T_{1/2}$. A sufficient amount of ventricular tissue for the analysis of electron microscopy was not obtained from all patients. In addition, follow-up data were not examined in this population, so we were not able to assess whether MIBI WR would be an independent predictor for disease severity or prognosis using a multivariate analysis. Furthermore, precise mitochondrial functions, such as mitochondrial respiration (e.g., intramyocellular triglyceride levels, respiratory exchange ratio, citrate synthase activity), were not directly assessed. These issues warrant further investigations in a larger population.

Although the association of focal MIBI WR with hemodynamic data is of interest, focal myocardial MIBI WR was not investigated. However, different from other cardiac diseases, a diffuse increase in washout is commonly observed in DCM. Because the present study aimed to investigate the relationship between global functional data and global scintigraphic parameters, we did not assess focal WR.

We cannot conclude an increase in mitochondrial density in more advanced cases, but this issue is very important and interesting. The mitochondrial density may increase in more advanced cases to compensate for the lack of cellular respiration. Meanwhile, we think that impaired glucose utilization in abnormal myocardium could result in an increase of glycogen-positive area in accordance with the mitochondrial impairment.

Ventricular biopsy specimens from six patients were available for electron microscopic analysis. Different from samples obtained from transplanted hearts, the quantity of biopsy specimens by bioptome is not sufficient for all PCR analyses, electron microscopic analyses, or standard histopathologic evaluations, such as myocardial fibrosis. Therefore, it is difficult to analyze electron microscopy in all patients.

We obtained scintigraphic parameters from normal control subjects. However, because we could not perform invasive cardiac catheter studies in normal control subjects for ethical reasons, we were unable to obtain their hemodynamic data,

and so we could not compare the hemodynamic data between normal control subjects and DCM patients.

Conclusions

An increased MIBI WR in DCM patients may predict mitochondrial dysfunction and the impairment in myocardial contractile and relaxation reserves during dobutamine stress. Our results may well lead to clinically useful findings to assume the responses to the optical medical treatments or patient prognoses. However, further studies are needed to clarify these issues in a larger population.

REFERENCES

1. Kelly DP, Strauss AW. Inherited cardiomyopathies. N Engl J Med 1994;330:913–9.
2. Dec GW, Fuster V. Idiopathic dilated cardiomyopathy. N Engl J Med 1994;331:1564–75.
3. Piwnica-Worms D, Chiu ML, Kronauge JF. Divergent kinetics of ^{201}Tl and ^{99m}Tc-sestamibi in cultured chick ventricular myocytes during atp depletion. Circulation 1992;85:1531–41.
4. Carvalho PA, Chiu ML, Kronauge JF, et al. Subcellular distribution and analysis of technetium-99m-MIBI in isolated perfused rat hearts. J Nucl Med 1992;33:1516–22.
5. Li QS, Frank TL, Franceschi D, et al. Technetium-99m methoxy-isobutyl isonitrile (rp30) for quantification of myocardial ischemia and reperfusion in dogs. J Nucl Med 1988;29:1539–48.
6. Liu Z, Okada DR, Johnson G, et al. ^{99m}Tc-sestamibi kinetics predict myocardial viability in a perfused rat heart model. Eur J Nucl Med Mol Imaging 2008;35:570–8.
7. Chiu ML, Kronauge JF, Piwnica-Worms D. Effect of mitochondrial and plasma membrane potentials on accumulation of hexakis (2-methoxyisobutylisonitrile) technetium(i) in cultured mouse fibroblasts. J Nucl Med 1990;31:1646–53.
8. Piwnica-Worms D, Kronauge JF, Chiu ML. Uptake and retention of hexakis (2-methoxyisobutyl isonitrile) technetium(i) in cultured chick myocardial cells. Mitochondrial and plasma membrane potential dependence. Circulation 1990;82:1826–38.
9. Fujiwara S, Takeishi Y, Hirono O, et al. Reverse redistribution of ^{99m}Tc-sestamibi after direct percutaneous transluminal coronary angioplasty in acute myocardial infarction: relationship with wall motion and functional response to dobutamine stimulation. Nucl Med Commun 2001;22:1223–30.
10. Takeishi Y, Sukekawa H, Fujiwara S, et al. Reverse redistribution of technetium-99m-sestamibi following direct PTCA in acute myocardial infarction. J Nucl Med 1996;37:1289–94.
11. Sugiura T, Takase H, Toriyama T, et al. Usefulness of Tc-99m methoxyisobutylisonitrile scintigraphy for evaluating congestive heart failure. J Nucl Cardiol 2006;13:64–8.

12. Kumita S, Seino Y, Cho K, et al. Assessment of myocardial washout of Tc-99m-sestamibi in patients with chronic heart failure: comparison with normal control. Ann Nucl Med 2002;16:237–42.

13. Matsuo S, Nakae I, Tsutamoto T, et al. A novel clinical indicator using Tc-99m sestamibi for evaluating cardiac mitochondrial function in patients with cardiomyopathies. J Nucl Cardiol 2007;14:215–20.

14. Ikawa M, Kawai Y, Arakawa K, et al. Evaluation of respiratory chain failure in mitochondrial cardiomyopathy by assessments of ^{99m}Tc-MIBI washout and ^{123}I-BMIPP/^{99m}Tc-MIBI mismatch. Mitochondrion 2007;7:164–70.

15. Unno K, Isobe S, Izawa H, et al. Relation of functional and morphological changes in mitochondria to myocardial contractile and relaxation reserves in asymptomatic to mildly symptomatic patients with hypertrophic cardiomyopathy. Eur Heart J 2009;30:1853–62.

16. Isobe S, Ohshima S, Unno K, et al. Relation of ^{99m}Tc-sestamibi washout with myocardial properties in patients with hypertrophic cardiomyopathy. J Nucl Cardiol 2010;17:1082–90.

17. Elliott P, Andersson B, Arbustini E, et al. Classification of the cardiomyopathies: a position statement from the European Society Of Cardiology Working Group on Myocardial and Pericardial Diseases. Eur Heart J 2008;29:270–6.

18. Schiller NB, Shah PM, Crawfold M, et al, for the American Society of Echocardiography Committee on Standards, Subcommittee on Quantitation of Two-Dimensional Echocardiograms. Recommendations for quantitation of the left ventricle by two-dimensional echocardiography. J Am Soc Echocardiogr 1989;2:358–67.

19. Kobayashi M, Izawa H, Cheng XW, et al. Dobutamine stress testing as a diagnostic tool for evaluation of myocardial contractile reserve in asymptomatic or mildly symptomatic patients with dilated cardiomyopathy. J Am Coll Cardiol Img 2008;1:718–26.

20. Hirashiki A, Izawa H, Cheng XW, Unno K, Ohshima S, Murohara T. Dobutamine-induced mechanical alternation is a marker of poor prognosis in idiopathic dilated cardiomyopathy. Clin Exp Pharmacol Physiol 2010;37:1004–9.

21. Sakakibara M, Hirashiki A, Cheng XW, et al. Association of diabetes mellitus with myocardial collagen accumulation and relaxation impairment in patients with dilated cardiomyopathy. Diabetes Res Clin Pract 2011;92:348–55.

22. Humphries KM, Yoo Y, Szweda LI. Inhibition of nadh-linked mitochondrial respiration by 4-hydroxy-2-nonenal. Biochemistry 1998;37:552–7.

23. Li Y, Park JS, Deng JH, Bai Y. Cytochrome c oxidase subunit IV is essential for assembly and respiratory function of the enzyme complex. J Bioenerg Biomembr 2006;38:283–91.

24. Arbustini E, Diegoli M, Fasani R, et al. Mitochondrial dna mutations and mitochondrial abnormalities in dilated cardiomyopathy. Am J Pathol 1998;153:1501–10.

25. Chen LB. Mitochondrial membrane potential in living cells. Annu Rev Cell Biol 1988;4:155–81.

26. Schaper J, Froede R, Hein S, et al. Impairment of the myocardial ultrastructure and changes of the cytoskeleton in dilated cardiomyopathy. Circulation 1991;83:504–14.

27. Szczepaniak LS, Dobbins RL, Metzger GJ, et al. Myocardial triglycerides and systolic function in humans: in vivo evaluation by localized proton spectroscopy and cardiac imaging. Magn Reson Med 2003;49:417–23.

28. Kitaoka H, Takata J, Yabe T, Hitomi N, Furuno T, Doi YL. Low dose dobutamine stress echocardiography predicts the improvement of left ventricular systolic function in dilated cardiomyopathy. Heart 1999;81:523–7.

29. Scrutinio D, Napoli V, Passantino A, Ricci A, Lagioia R, Rizzon P. Low-dose dobutamine responsiveness in idiopathic dilated cardiomyopathy: relation to exercise capacity and clinical outcome. Eur Heart J 2000;21:927–34.

30. Ohshima S, Isobe S, Izawa H, et al. Cardiac sympathetic dysfunction correlates with abnormal myocardial contractile reserve in dilated cardiomyopathy patients. J Am Coll Cardiol 2005;46:2061–8.